

Multi-electron Redox Reactions with Iron and Vanadium Ions at a Mixed Phosphate-Sulfate during Sodium Intercalation

Violeta Koleva, Trajche Tushev, Sonya Harizanova, Rositsa Kukeva, Maria Shipochka, Pavel Markov and Radostina Stoyanova*

Institute of General and Inorganic Chemistry, Bulgarian Academy of Sciences, Acad. G. Bonchev Str., Bldg. 11, 1113 Sofia, Bulgaria

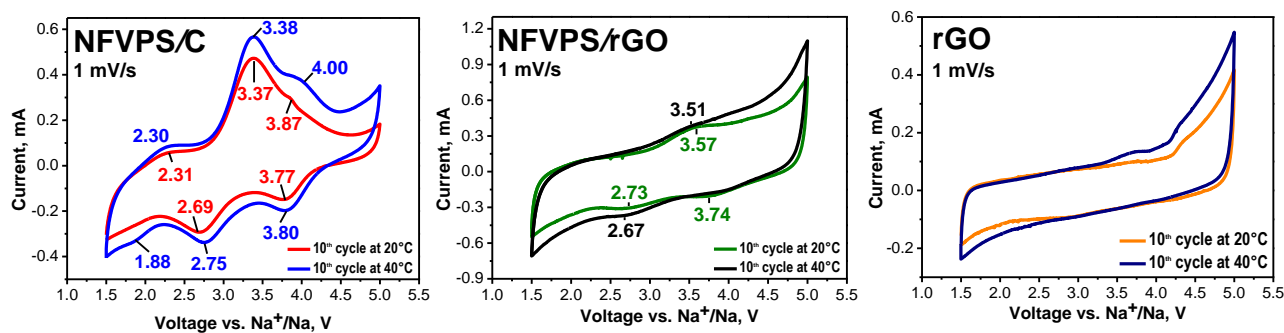


Fig. S1. CV curves of NFVPS/C, NFVPS/rGO and rGO in sodium half-cells at a scanning rate of 1 mV/s within voltage window between 1.5 and 5.0 V (20 and 40 °C).

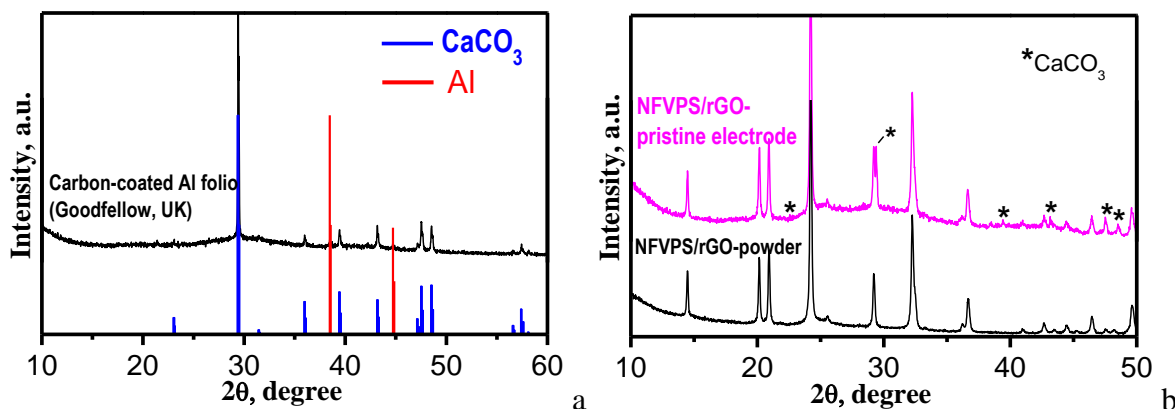


Fig. S2. (a) XRD pattern of the carbon-coated Al folio used (Goodfellow, Cambridge Ltd., UK). Red bars correspond to reference pattern of aluminium (COD-96-900-8461) and blue bars - to calcite CaCO_3 (COD-96-154-7348); (b) XRD patterns of powder NFVPS/rGO and pristine electrode, where the asterisks denote the peaks due to CaCO_3 from plastic holder.

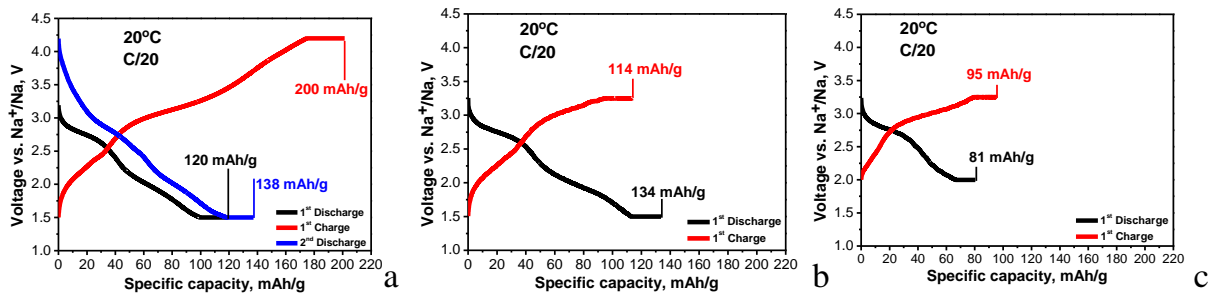


Fig. S3. Charge-discharge curves with a C/20 rate in different voltage windows (20 °C): (a) between 1.5 and 4.2 V; (b) between 1.5 and 3.25 ; (c) between 2.0 and 3.25 V. The cells start with a discharge mode and are kept at discharged and charged state for 10 hr. The numbers in the figure correspond to the specific capacities obtained at given potential before and after holding for 10 hs.

Table S1. Lattice parameters of NFVPS, NFVPS/rGO and electrodes cycled in Na half-cells with NaPF₆/PC electrolyte and stopped at different voltages

| Description Electrode composition | <i>a</i> (Å) | <i>c</i> (Å) | <i>V</i> (Å ³) | <i>ΔV</i> (%)* |
|--|----------------|--------------|----------------------------|----------------|
| NFVPS-powder | 8.4691(1) | 22.0162(1) | 1367.58(12) | |
| NFVPS/rGO-powder NaFeVPO₄(SO₄)₂ | 8.4811(1) | 21.9907(1) | 1369.86(18) | |
| Pristine electrode NFVPS/rGO NaFeVPO₄(SO₄)₂ | 8.4936(2) | 21.9867(4) | 1373.6(2) | 0 |
| 1 st charge to 4.2 V (C/20 rate, 20 °C) Na_{0.40}FeVPO₄(SO₄)₂ | 8.504(1) | 21.967 (4) | 1377.7 | + 0.15 |
| 1 st charge to 4.2 V and discharge to 1.5 V (C/20 rate, 20 °C) Na_{2.8}FeVPO₄(SO₄)₂ | 8.640(3) | 22.084(9) | 1427.9(9) | + 3.8 |
| 1 st charge to 4.2 V and discharge to 1.5 V and 2 nd charge to 4.2 V (C/20 rate, 20 °C) Na_{0.6}FeVPO₄(SO₄)₂ | 8.4932(1) | 21.956(4) | 1371.6(4) | - 0.1 |
| 1 st discharge to 1.5 V (C/20 rate, 20 °C) Na_{2.8}FeVPO₄(SO₄)₂ | 8.699(2) | 22.04(1) | 1444.3(9) | + 5.1 |
| 1 st discharge to 1.5V and charge to 4.2V (C/20 rate, 20 °C) Na₀FeVPO₄(SO₄)₂ | 8.5037(3) | 21.9465(5) | 1374.3(2) | + 0.05 |
| 1 st discharge to 1.5 V, charge to 4.2 V and 2 nd discharge to 1.5 V (C/20 rate, 20 °C) Na_{2.1}FeVPO₄(SO₄)₂ | 8.6596(1) - | 22.0506(1) | 1432.30(5) | + 4.0 |
| 1 st discharge to 2.0 V and charge to 3.25 V (C/20 rate, 20 °C) Na_{0.8}FeVPO₄(SO₄)₂ | 8.526(2) | 21.950(3) | 1380.8(9) | + 0.5 |
| 1 st discharge to 1.5 V and charge to 3.25 V (C/20 rate, 20 °C) Na_{1.3}FeVPO₄(SO₄)₂ | 8.513(3) | 21.950(2) | 1377.0(7) | + 0.3 |
| Discharged electrode (1.5 V) after 200 cycles (100 cycles at 20°C and subsequent 100 cycles at 40 °C with C/2 rate); start with a charge mode | 8.5088 | 21.968(2) | 1377.4(2) | + 0.3 |

| | | | | |
|---|-----------|------------|-----------|------|
| Charged electrode (4.5 V) after 200 cycles (100 cycles at 20°C and subsequent 100 cycles at 40 °C with C/2 rate); start with a discharge mode | 8.450(2) | 21.931(2) | 1356.1(8) | -1.2 |
| Discharged electrode (1.5 V) after 100 cycles at 40 °C with C/2 rate; start with a charge mode | 8.5173(4) | 21.9604(6) | 1379.6(3) | +0.4 |

* ΔV is calculated in respect to the pristine electrode

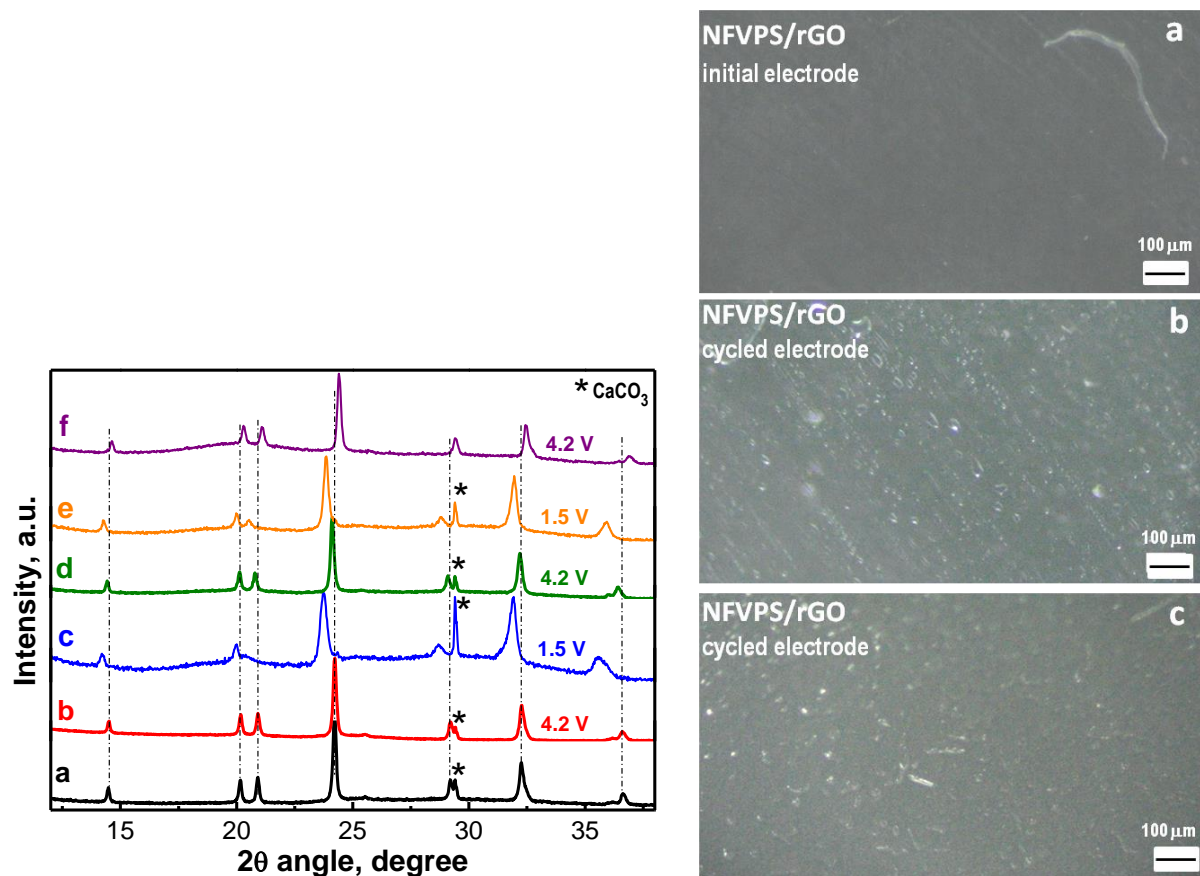


Fig. S4. (left) *Ex-situ* XRD patterns of electrodes cycled between 1.5 and 4.2V and stopped at discharged or charged state: (a) pristine electrode; (b) 1st charge to 4.2 V at 20 °C (point 1 in Fig. 4a); (c) 1st discharge to 1.5 V at 20 °C (point 1' in Fig. 4c); (d) charged electrode after 1st discharge at 20 °C (point 2' in Fig. 4c); (e) 2nd discharge at 20 °C (point 3' in Fig. 4c); (f) charged electrode after 1st discharge at 40 °C; (right) Optical images of pristine NFVPS/rGO electrode (a) and after cycling at C/2 rate for 200 cycles (100 cycles at 20 °C and subsequent 100 cycles at 40 °C) when the cell starts with a charge mode (b) and with a discharge mode (c).

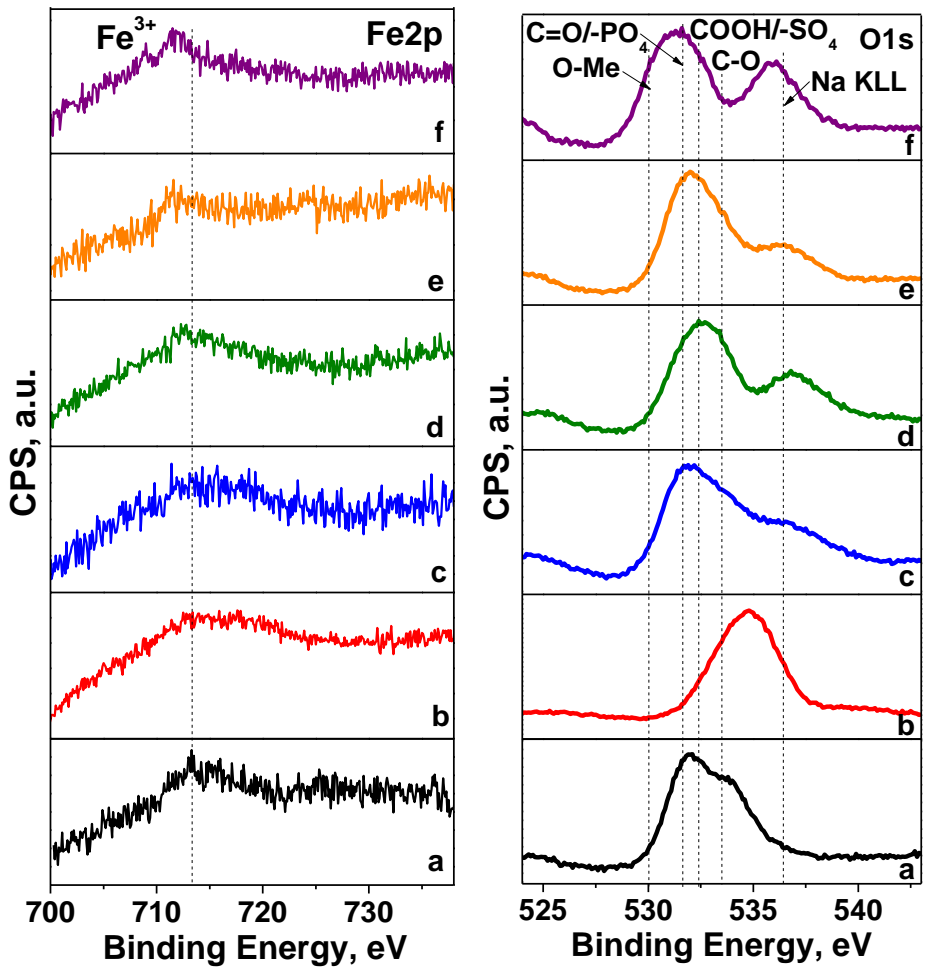


Fig. S5. XPS spectra in the regions of Fe2p and O1s binding energies of electrodes cycled between 1.5 and 4.2 V and stopped at discharge or charged state: (a) pristine electrode; (b) 1st charge to 4.2 V at 20 °C (point 1 in Fig. 4a); (c) 1st discharge to 1.5 V at 20 °C (point 1' in Fig. 4c); (d) charged electrode after 1st discharge at 20 °C (point 2' in Fig. 4c); (e) 2nd discharge at 20 °C (point 3' in Fig. 4c); (f) charged electrode after 1st discharge at 40 °C.

Table S2. Element content of the electrodes determined from XPS spectra

| № | Sample description | Element content, at. % | | | | | | | | |
|---|--|------------------------|-----|-----|-----|-----|------|------|------|--|
| | | Na | Fe | V | P | S | O | C | F | |
| 1 | pristine NFVPS electrode | 1.2 | 1.3 | 1.3 | 2.4 | 1.5 | 21.1 | 54.9 | 16.3 | |
| 2 | 1 st charge to 4.2 V at 20 °C (point 1 in Fig. 4a) | 3.9 | 2.6 | 0.5 | 4.3 | 1.8 | 32.8 | 24.9 | 29.2 | |
| 3 | 1 st discharge to 1.5 V at 20 °C (point 1' in Fig. 4c) | 15.9 | 1.9 | 0.8 | 4.8 | 0.4 | 31.5 | 24.5 | 20.2 | |
| 4 | charged electrode after 1 st discharge at 20 °C (point 2' in Fig. 4c) | 10.6 | 1.6 | 0.4 | 5.7 | 0.8 | 26.1 | 29.6 | 25.2 | |
| 5 | 2 nd discharge at 20 °C (point 3' in Fig. 4c) | 16.2 | 0.7 | 0.4 | 2.8 | 0.9 | 35.5 | 32.2 | 11.3 | |
| 6 | charged electrode after 1 st discharge at 40 °C | 16.2 | 1.8 | 0.2 | 4.8 | 0.2 | 22.9 | 28.6 | 25.3 | |

Table S3. Percentages of the different components of the C peaks.

| № | Chemical bonding | C-C | C-O | C=O | C-F, COOH | CF ₂ | CF ₃ | $\frac{C-C}{C-O}$ | $\frac{C-C}{C=O}$ |
|------------------|--|--------------------|-------|-------|--------------|-----------------|-----------------|-------------------|-------------------|
| | | Binding energy, eV | 285.0 | 286.4 | 287.7 | 289.0 | 290.8 | 292.8 | |
| Concentration, % | | | | | | | | | |
| 1 | pristine NFVPS electrode | 45.3 | 22.1 | 13.1 | 5.9 | 11.8 | 1.8 | 2.05 | 3.46 |
| 2 | 1 st charge to 4.2 V at 20 °C (point 1 in Fig. 4a) | 25.5 | 25.0 | 22.2 | 11.8 | 11.0 | 4.5 | 1.02 | 1.15 |
| 3 | 1 st discharge to 1.5 V at 20 °C (point 1' in Fig. 4c) | 51.9 | 23.3 | 13.1 | 11.1 | 10.7 | 7.2 | 2.23 | 3.96 |
| 4 | charged electrode after 1 st discharge at 20 °C (point 2' in Fig. 4c) | 51.9 | 28.2 | 13.6 | 11.7 | 4.0 | - | 1.84 | 3.82 |
| 5 | 2 nd discharge at 20 °C (point 3' in Fig. 4c) | 53.8 | 13.5 | 10.4 | 9.8 | 8.6 | 3.9 | 3.99 | 5.17 |
| 6 | charged electrode after 1 st discharge at 40 °C | 51.9 | 15.5 | 19.1 | 10.5 | 3.0 | - | 3.35 | 2.72 |

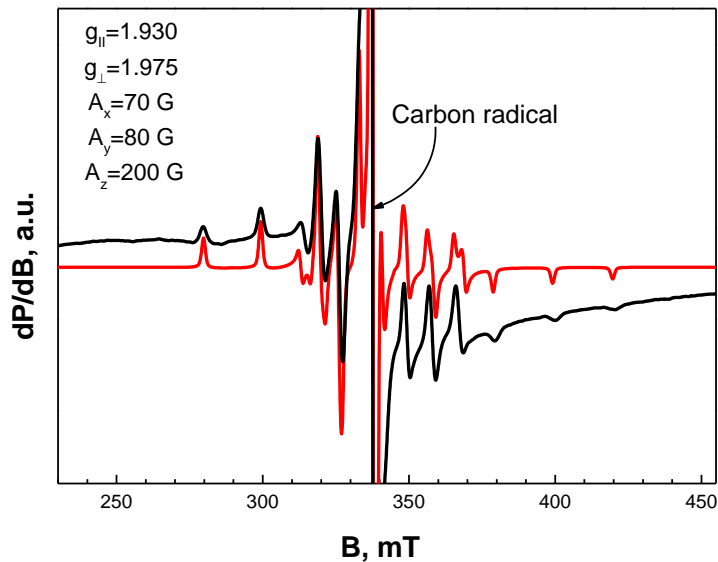


Fig. S6. EPR spectrum after the subtraction of the signal due to Fe³⁺ ions for the step-wise cycled electrode (20 and 40 °C for 200 cycles in total) that is stopped at discharged state. The red line corresponds to the simulated multiplet signal. The signal due to carbon additives is also shown.

Table S4. Spin-Hamiltonian parameters of VO^{2+} ions in various crystal lattices

| Nº | Lattice | \mathbf{g}_{\parallel} | \mathbf{g}_{\perp} | $A_{\parallel}, [\text{G}]$ | $A_{\perp}, [\text{G}]$ |
|-----------|---|--|--|---|---|
| 1 | Pristine NFVPS electrode [this work] | $g_z=1.930$ | $g_{\perp}=1.974$ | $A_z=200$ | $A_x=80$ $A_y=70$ |
| 2 | $\text{ZnSO}_4 \cdot 7\text{H}_2\text{O}$ single crystals [1] | $g_z=1.945$ | $g_x=1.986$ $g_y=1.985$ | $A_z=206$ | $A_x=76.9$ $A_y=79.4$ |
| 3 | $\text{GdNa}_2(\text{SO}_4)_2 \cdot 6\text{H}_2\text{O}$ (CSSH) single crystals [2] | $g_z=1.938$ | $g_x=1.984$ $g_y=1.975$ | $A_z=186$ | $A_x=65.6$ $A_y=75.0$ |
| 4 | $(\text{NH}_4)_2\text{SO}_4$ single crystals [3] | $g_z=1.930$ | $g_x=1.976$ $g_y=1.982$ | $A_z=192.2$ | $A_x=73$ $A_y=77$ |
| 5 | $\text{ZnTiF}_6 \cdot 6\text{H}_2\text{O}$ single crystals [4] | $g_z=1.946$ | $g_{\perp}=1.988$ | $A_z=197$ | $A_{\perp}=80$ |
| 6 | $\text{Gd}_2\text{ZrF}_8 \cdot 6\text{H}_2\text{O}$ single crystals [5] | $g_z=1.935$ | $g_{\perp}=1.981$ | $A_z=197$ | $A_{\perp}=82$ |
| 7 | $(\text{NH}_4)_3\text{AlF}_6$ single crystals [6] | $g_z=1.937$ | $g_{\perp}=1.977$ | $A_z=190$ | $A_{\perp}=68$ |
| 8 | Alkali barium phosphate glasses [7] | $g_z=1.920-1.925$ | $g_{\perp}=1.974-1.977$ | $A_z=190-192$ | $A_x=72-73$ $A_y=83-85$ |
| 9 | $\text{CdNH}_4\text{PO}_4 \cdot 6\text{H}_2\text{O}$ single crystals [8] | $g_z=1.931$ | $g_{\perp}=1.993$ | $A_z=195$ | $A_{\perp}=77$ |
| 10 | KH_2PO_4 single crystals [9] | $g_z=1.924-1.935$ | $g_{\perp}=1.992-1.998$ | $A_z=192-207$ | $A_{\perp}=80-91$ |

- [1] A. K. Viswanath. EPR studies of VO^{2+} in single crystals of $\text{ZnS}0_4 \cdot 7\text{H}_2\text{O}$ and certain polycrystalline sulfates. *J. Chem. Phys.* 67 (1977) 3744. DOI:10.1063/1.435315.
- [2] C. Shiyamala, S. Mithira, B. Natarajan, R. V. S. S. N. Ravikumar, P. Sambasiva Rao. Site determination of vanadyl impurity in cadmium sodium sulphate hexahydrate: single crystal EPR and optical studies. *Phys. Scr.* 74 (2006) 549–554. DOI: 10.1088/0031-8949/74/5/011.
- [3] S.D. Pandey, P. Enkateswarlu. Electron paramagnetic resonance of vanadyl-doped ammonium sulfate single crystals. *J. Magn. Reson.* 17 (1975) 137-150.
- [4] G. Jayaram, V. G. Krishnan. EPR of VO^{2+} in $\text{ZnTiF}_6 \cdot 6\text{H}_2\text{O}$. *Z. Naturforsch. A.* 51a (1996) 245-248. DOI:10.1515/zna-1996-0403.
- [5] G. Jayaram, V. G. Krishnan. EPR of VO^{2+} doped $\text{Cd}_2\text{ZrF}_8 \cdot 6\text{H}_2\text{O}$ in single crystals. *Z. Naturforsch.* 50a (1995) 953-956. DOI:10.1515/zna-1995-1008
- [6] P. T. Manoharam, M. T. Rogers. ESR study of VF_5^{3-} ion. *J. Chem. Phys.* 49 (1968) 3912-3918. <https://doi.org/10.1063/1.1670700>.
- [7] V. R. Kumar, R. P. S. Chakradhar, A. Murali, N. O. Gopal, J. L. Rao. A study of electron paramagnetic resonance and optical absorption spectra of VO^{2+} ions in alkali barium phosphate glasses. *Int. J. Mod. Phys. B* 17 (2003) 3033-3047. DOI: 10.1142/S0217979203020703
- [8] I. Sougandi, T. M. Rajendiran, R. Venkatesan, P. S. Rao. Single crystal EPR study of VO(II)-doped cadmium potassium phosphate hexahydrate: A substitutional incorporation. *Proc. Indian Acad. Sci. (Chem. Sci.)*, 114 (2002) 473-479.
- [9] R. Biyik, R. Tapramaz, EPR and Optical Absorption Studies of VO^{2+} doped KH_2PO_4 and $\text{KH}_3\text{C}_4\text{O}_8 \cdot 2\text{H}_2\text{O}$ single crystals. *Z. Naturforsch.* 61a (2006) 171-179.